Effects of the substituents of pyrazole/thiazine ligands on nuclearity of Cu(II) nitrate complexes

P. Torres-García [a], E. VIÑUelas-Zahínos [a], F. Luna-Giles [a] & A. Bernalte-García [a]

[a] Department of Organic and Inorganic Chemistry, University of Extremadura, 06071 Badajoz, Spain
Accepted author version posted online: 07 Aug 2012. Published online: 03 Sep 2012.

PLEASE SCROLL DOWN FOR ARTICLE

Effects of the substituents of pyrazole/thiazine ligands on nuclearity of Cu(II) nitrate complexes

P. TORRES-GARCÍA, E. VIÑUELAS-ZAHÍNOS, F. LUNA-GILES*
and A. BERNALTE-GARCÍA

Department of Organic and Inorganic Chemistry, University of
Extremadura, 06071 Badajoz, Spain

$[Cu(H_2O)(PzTz)_2](NO_3)_2$ (**1**), $[Cu(\mu\text{-}NO_3)(NO_3)(DMPzTz)]_n$ (**2**), and $[\{Cu(NO_3)(DPhPzTz)\}_2 (\mu\text{-}NO_3)_2]$ (**3**) [PzTz = 2-(1-pyrazolyl)-1,3-thiazine, DMPzTz = 2-(3,5-dimethyl-1-pyrazolyl)-1,3-thiazine, DPhPzTz = 2-(3,5-diphenyl-1-pyrazolyl)-1,3-thiazine] have been prepared and characterized by elemental analysis, electronic spectroscopy, IR spectroscopy, electron paramagnetic resonance spectroscopy, magnetic susceptibility measurements, and single-crystal X-ray diffraction. Influence of ligand size on coordination to Cu(II) has been analyzed. The three complexes are five-coordinate and the coordination geometry can be described as a distorted trigonal bipyramid for **1** or a distorted square pyramid for **2** and **3**. As a consequence of the strain induced by the ligands, **1** is a monomeric complex cation whereas **2** is a polymer and **3** is a dimer.

Keywords: Copper(II) complexes; Pyrazole; Thiazine; Crystal structures; Nuclearity

1. Introduction

Polydentate ligands with *N,N* or *N,S* donors have been used in coordination chemistry toward transition metal ions, with special interest in biological systems [1]. The presence of heterocycles in new compounds can provide coordination versatility, since they can act as *N,N* or *S,N*-ligands through nitrogen from pyrazole and nitrogen or sulfur from thiazine, depending on the metal [2]. Our group recently developed some new pyrazole/1,3-thiazine ligands and started to study their coordination behavior toward d block metals, proving that different structural features in the ligand can cause differences in the coordination environment of the metal [3–5]. Expanding this research, we have investigated the role played by substituent's size in these ligands on nuclearity of several Cu(II) complexes, since this ion forms coordination compounds containing a variable number of metal centers, with a number of monomers, dimers, trimers, and polymers reported. In this article, we prepare and characterize three Cu(II) complexes with 2-(1-pyrazolyl)-1,3-thiazine (PzTz), 2-(3,5-dimethyl-1-pyrazolyl)-1,3-thiazine (DMPzTz), and 2-(3,5-diphenyl-1-pyrazolyl)-1,3-thiazine (DPhPzTz) (scheme 1) to

---

*Corresponding author. Email: pacoluna@unex.es
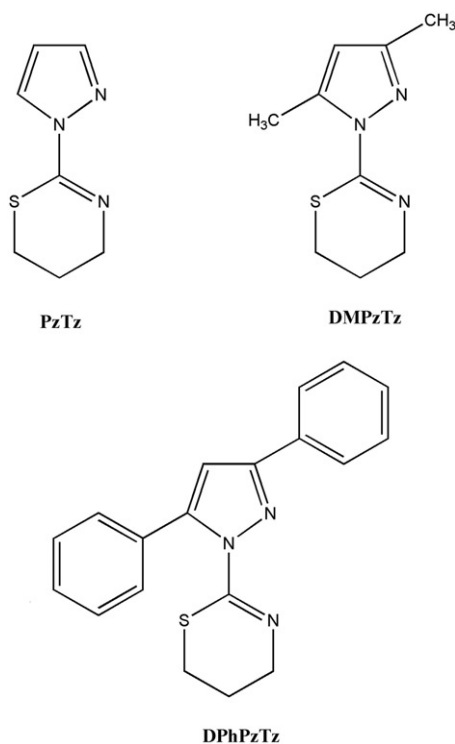
Scheme 1.   Organic ligand.

understand the structural factors that determine nuclearity in these complexes by varying substituents in positions 3 and 5 in the pyrazole ring. Results are reported on isolation of $[Cu(H_2O)(PzTz)_2](NO_3)_2$ (**1**), $[Cu(DMPzTz)(\mu\text{-}NO_3)(NO_3)]_n$ (**2**), and $[\{Cu(NO_3)(DPhPzTz)\}_2(\mu\text{-}NO_3)_2]$ (**3**) and characterization by elemental analysis, single-crystal X-ray diffraction, electronic spectra, IR spectra, electron paramagnetic resonance (EPR), and magnetic susceptibility measurements.

2. Experimental

2.1. *General procedures*

All reagents were of commercial grade material and used without any purification. PzTz, DMPzTz, and DPhPzTz were synthesized as previously reported [3]. Chemical analyses of carbon, hydrogen, nitrogen, and sulfur were performed by microanalytical methods using a Leco CHNS-932 microanalyser. IR spectra were recorded on a Thermo IR-300 spectrophotometer from KBr pellets ($4000–370\,cm^{-1}$) on a Perkin-Elmer FT-IR 1700X spectrophotometer and from Nujol mull in the $500–150\,cm^{-1}$ range. UV-Vis–NIR reflectance spectra for complexes in the 200–1400 nm range were obtained from pellets of the samples using a Shimadzu UV-3101 PC spectrophotometer

and $BaSO_4$ as a reference. EPR spectra were recorded at room temperature in the solid state employing a BRUKER ESP-300 E spectrometer using the X band. Magnetic susceptibility measurements were performed on polycrystalline samples using a magnetometer with a pendulum MANICS DSM8, equipped with helium continuous flow cryostat and an electromagnetometer DRUSCH EAF 16 UE. Data were corrected for temperature independent paramagnetism and diamagnetic contributions, which were estimated from the Pascal constants.

2.2. Synthesis of the complexes

Copper(II) complexes were prepared by reacting a solution (2 mL) of $Cu(NO_3)_2 \cdot 3H_2O$ (24.2 mg, 0.10 mmol) in methanol with a solution of the ligand in the same solvent, with a 1 : 1 metal–ligand molar ratio. As supporting of conclusions deduced for this work, syntheses for **2** and **3** have been repeated with a 1 : 2 metal–ligand ratio obtaining the same compounds as those isolated with a 1 : 1 metal–ligand ratio. X-ray quality crystals were obtained when the solution was surrounded with ether using a liquid-vapor diffusion method. The solids were filtered, washed with cold ether, and finally air-dried.

2.2.1. Synthesis of $[Cu(H_2O)(PzTz)_2](NO_3)_2$ (1). Yield: 46.0 mg, 85.1%. Anal. Calcd for $C_{14}H_{20}CuN_8O_7S_2$ (%): C, 31.13; H, 3.73; N, 20.75; S, 11.87. Found (%): C, 31.26; H, 3.74; N, 20.68; S, 11.93. IR (KBr): (sh = shoulder, w = weak, m = medium, s = strong, vs = very strong) thiazine ring vibrations 1606(vs) [ν(C=N)], 922(m), 896(m), 879(m), 604(m), 534(m), 428(m) cm^{-1}; pyrazole ring vibrations: 1527(s), 1425(s), 1382(vs), 1324(vs), 1008(s) cm^{-1}.

2.2.2. Synthesis of $[Cu(\mu-NO_3)(NO_3)(DMPzTz)]_n$ (2). Yield: 28.1 mg, 72.5%. Anal. Calcd for $C_9H_{13}CuN_5O_6S$ (%): C, 28.23; H, 3.40; N, 18.29; S, 8.36. Found (%): C, 28.41; H, 3.68; N, 18.33; S, 8.61. IR (KBr): thiazine ring vibrations 1602(s) [ν(C=N)], 983(sh), 908(m), 869(w), 748(m), 592(w), 553(sh), 445(w) cm^{-1}; pyrazole ring vibrations: 1565(s), 1382(vs), 1422(sh), 991(m) cm^{-1}.

2.2.3. Synthesis of $[\{Cu(NO_3)(DPhPzTz)\}_2(\mu-NO_3)_2]$ (3). Yield: 30.0 mg, 29.4%. Anal. Calcd for $C_{38}H_{34}Cu_2N_{10}O_{12}S_2$ (%): C, 45.01; H, 3.38; N, 13.81; S, 6.32. Found (%): C, 45.36; H, 3.69; N, 13.54; S, 6.59. IR (KBr): thiazine ring vibrations 1614(s) [ν(C=N)], 964(m), 923(w), 877(w), 763(m), 593(w), 539(w), 460(w) cm^{-1}; pyrazole ring vibrations: 1554(m), 1411(m), 1311(s), 1006(m) cm^{-1}.

2.3. Crystal structures determination

X-ray diffraction measurements were performed using a Bruker APEX or a Bruker SMART CCD diffractometer with Mo-Kα radiation ($\lambda = 0.71073$ Å, graphite monochromator). Absorption corrections were applied using SADABS [6]. The structures were solved by direct methods and subsequent Fourier differences using SHELXS-97 [7] and refined by full-matrix least-squares on F^2 with SHEXL-97 [8], included in WINGX package [9], assuming anisotropic displacement parameters for non-hydrogen atoms.

Table 1. Crystal data and structure refinement details for **1–3**.

	1	**2**	**3**
Crystal shape	Prism	Prism	Prism
Color	Blue	Blue	Green
Crystal size (mm^3)	$0.24 \times 0.14 \times 0.14$	$0.16 \times 0.10 \times 0.06$	$0.54 \times 0.22 \times 0.09$
Empirical formula	$C_{14}H_{20}CuN_8O_7S_2$	$C_9H_{13}CuN_5O_6S$	$C_{38}H_{34}Cu_2N_{10}O_{12}S_2$
Formula weight	540.04	382.84	1013.95
Crystal system	Monoclinic	Orthorhombic	Triclinic
Space group	$I2/a$	$P2_12_12_1$	$P\bar{1}$
Unit cell dimensions (Å, °)			
a	14.578(4)	8.671(1)	10.217(3)
b	7.295(2)	11.029(1)	10.637(3)
c	19.760(6)	14.482(1)	10.930(3)
α			102.762(4)
β	102.503(5)		116.710(3)
γ			93.110(4)
Volume ($Å^3$), Z	2051.4(10), 4	1385.0(1), 4	3658(3), 1
Temperature (K)	110(2)	100(2)	100(2)
Calculated density ($g\,cm^{-3}$)	1.749	1.836	1.653
Absorption coefficient (mm^{-1})	1.326	1.767	1.224
$F(000)$	1108	780	518
θ range for data collection (°)	2.1–26.4	2.3–25.3	2.0–26.4
Index range	$-18 \le h \le 17$;	$-10 \le h \le 10$;	$-12 \le h \le 11$;
	$0 \le k \le 9$;	$0 \le k \le 13$;	$-13 \le k \le 12$;
	$0 \le l \le 24$	$0 \le l \le 17$	$0 \le l \le 13$
Independent reflection	2104 [$R(int) = 0.039$]	2533 [$R(int) = 0.051$]	4140 [$R(int) = 0.028$]
Observed reflection $[F > 4.0\,\sigma(F)]$	1636	2263	3567
Data completeness	0.999	0.999	0.994
Max. and min. transmission	0.836 and 0.741	0.901 and 0.765	0.898 and 0.558
No. of ref. parameters	146	201	289
R $[F > 4.0\,\sigma(F)]^a$	0.037	0.031	0.027
wR $[F > 4.0\,\sigma(F)]^b$	0.085	0.053	0.064
Goodness-of-fit on F^2 (GOF)^c	1.086	1.024	1.067
ρ_{max} and ρ_{min} (e Å^{-3})	0.92 and -0.538	0.26 and -0.355	0.312 and -0.376

$^a R = \Sigma ||F_o| - |F_c||/\Sigma |F_o|$.

$^b R = \left\{ \Sigma \left[w \left(F_o^2 - F_c^2 \right)^2 \right] / \Sigma \left[w \left(F_o^2 \right)^2 \right] \right\}^{1/2}$.

$^c \text{GOF} = \left\{ \Sigma \left[w \left(F_o^2 - F_c^2 \right)^2 \right] / \left(N_{rflns} - N_{params} \right) \right\}^{1/2}$.

All hydrogen atoms were positioned geometrically with U_{iso} values derived from U_{eq} values of the corresponding carbon or oxygen. Graphical representations of the molecular structures were generated using ORTEP3 [10] and Mercury [11] for Windows. Experimental details of the crystal structure determinations are listed in table 1.

3. Results and discussion

3.1. *Crystal structures*

Complex **1** contains four $[Cu(H_2O)(PzTz)_2]^{2+}$ cations and eight NO_3^- in its monoclinic unit cell, therefore the complex salt can be formulated as $[Cu(H_2O)(PzTz)_2](NO_3)_2$ (**1**). In table 2, the most relevant bond lengths and angles are listed, whereas figure 1 shows a

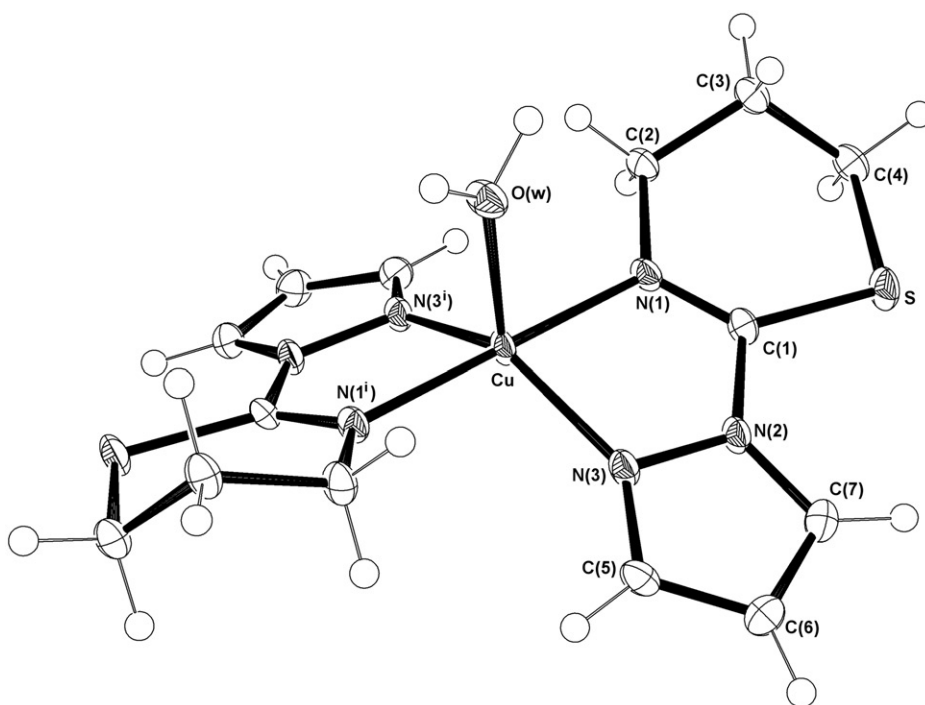Figure 1. Molecular structure of $[Cu(H_2O)(PzTz)_2]^{2+}$ in **1**. The thermal ellipsoids are plotted at the 50% probability level and hydrogen atoms are included as spheres of arbitrary radii.

representation of the structure of the complex cation. In the complex cation, Cu(II) is bonded to one water molecule and two PzTz ligands which coordinate through pyrazole and thiazine nitrogen atoms, forming a five-membered chelate ring. According to the methods proposed by Addison [12] and by Muetterties and Guggemberger [13] to determinate the coordination geometry of five-coordinate complexes, the values obtained for τ (0.61) and Δ (0.40) indicate that the coordination polyhedron around the copper atom can be described as a highly distorted trigonal bipyramid. The equatorial positions in this bipyramid are occupied by O(1w), N(3), and N(3^i), whereas the axial positions correspond to N(1) and N(1^i).

The structure of **2** is constituted by polymeric chains parallel to the crystallographic *a*-axis formed by $[Cu(\mu\text{-}NO_3)(NO_3)(DMPzTz)]$ units linked to each other with bridging nitrates. Figure 2 shows the structure of the complex and table 3 contains the most important bond distances and angles. Each copper is five-coordinate, bonded to the pyrazole and thiazine nitrogen atoms of one DMPzTz, the oxygen O(1) of a terminal nitrate, and two oxygen atoms of two bridging nitrates O(4) and O(5^i). The ligand geometry around copper(II) is best described as a square pyramid ($\tau = 0.15$, $\Delta = 0.85$). The Cu is situated 0.203 Å from the mean plane formed by the four base atoms N(1), N(3), O(1), and O(4) toward the apical O(5^i). However, the oxygen atom O(6) from one bridging nitrate group, which is situated at 2.727(2) Å from the copper(II) ion, could occupy the sixth coordination position to give a $(4 + 1 + 1^*)$-type coordination [14–16].
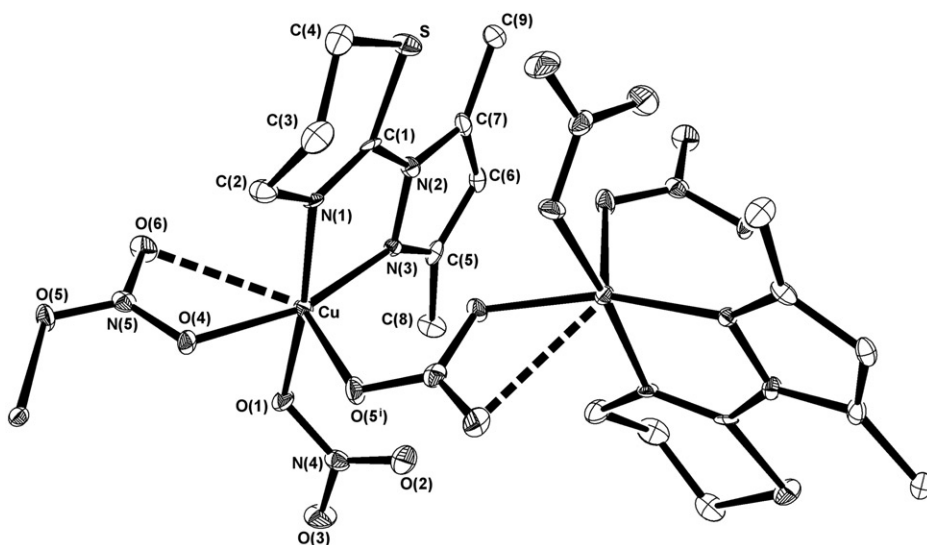
Figure 2.   Fragment of the structure of **2**. Thermal ellipsoids are plotted at the 50% probability level and hydrogen atoms are omitted for clarity.

Table 2. Selected bond distances (Å), angles (°), and hydrogen-bond parameters for **1**.

Cu–N(1)	1.989(3)	Cu–N(3)	1.999(3)
Cu–O(w)	2.183(3)		
N(1)–Cu–N(3)	81.1(1)	N(1)–Cu–O(w)	90.2(1)
N(1)–Cu–N(1^i)	179.7(2)	N(1)–Cu–N(3^i)	98.8(1)
N(3)–Cu–O(w)	108.6(1)	N(3)–Cu–N(3^i)	142.9(2)
D–H$\cdots$A	Position of A	A$\cdots$D (Å)	A$\cdots$H–D (°)
O(w)–H$\cdots$O(1)	*x, y, z*	2.801(26)	168(2)

Symmetry code: $^i 1/2 - x, y, -z$.

The structure of **3** consists of dimeric molecules $[\{Cu(NO_3)(DPhPzTz)\}_2(\mu\text{-}NO_3)_2]$ like the one represented in figure 3. Selected bond lengths and angles are indicated in table 3. The two Cu(II) centers are linked by two bridging monodentate nitrates, forming a four-membered ring plane with an inversion center. Each copper is further coordinated to one bidentate DPhPzTz and to oxygen of one terminal nitrate. The coordination geometry can be described as a distorted square pyramid, according to Addison *et al.* ($\tau = 0.20$) and to Muetterties and Guggemberger ($\Delta = 0.83$), with the apical position occupied by O(4^i) and N(1), N(3), O(1) and O(4) in the basal positions. Similar to **2**, O(2) from the terminal nitrate situated at a potential bond distance of 2.808 Å could be occupying the sixth position to give a $(4 + 1 + 1^*)$ coordination.

The copper(II)-ligand bond distances in **1**–**3** have been compared with the average value calculated for similar compounds found in the Cambridge Structural Database (CSD) [17]. The Cu–N$_{pyrazole}$ bond distance in **1** is similar to the mean value 2.008(90) Å calculated for 51 five-coordinate Cu(II) complexes with a CuN$_4$O chromophore
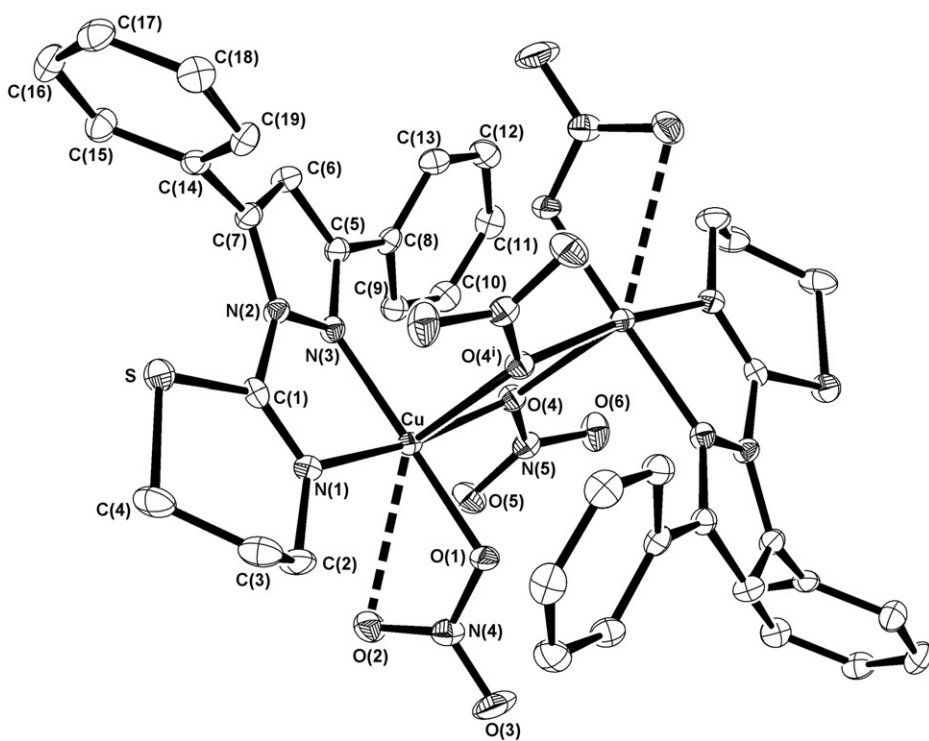
Figure 3. Molecular structure of **3**. Thermal ellipsoids are plotted at the 50% probability level and hydrogen atoms are omitted for clarity.

presenting this kind of union. Likewise, the Cu–OH$_2$ bond length is the same order as the average value [2.24(16) Å] corresponding to 250 five-coordinate copper(II) compounds with the same environment. On the other hand, Cu–(ONO$_2$)$_{terminal}$ and Cu–(ONO$_2$)$_{bridge}$ bond distances in **2** are in agreement with those of the polymers catena-{[μ_3-N,N'-[2,4-di((dipyridin-2-yl)amine)-1,3,5-triazin-6-yl]ethylenediamine]-(μ_2-nitrato)-(nitrato-O,O')-tetrakis(nitrato)-tri-copper(II)} [18] and catena-{bis[μ_3-2,4,6-tris(dipiridin-2-ylamine)-1,3,5-triazine]-bis-(μ_2-nitrato)-bis(acetonitrile)-octakis(nitrato)-penta-copper(II)} [19], found in CSD, in which the copper has an N$_2$O$_3$ environment and is bonded to two monodentate and one bridging nitrate [Cu–(ONO$_2$)$_{terminal}$: 1.950(2) Å and 1.996(4) Å; Cu–(ONO$_2$)$_{bridge}$: 2.288(4) Å and 2.378(2) Å]. For **3**, the long Cu–(O–NO$_2$)$_{bridge}$ distance is slightly longer and the short one is similar to those found in CSD for three dimeric Cu(II) compounds with two bridging and one terminal nitrates and chromophore CuN$_2$O$_3$: bis-[(μ_2-nitrato-O,O)-(1,1'-ditrithyl-4,4'-biimidazole)-nitrato-copper(II)]acetonitrile solvate [20], bis-[(μ_2-nitrato-O,O)-(2,2'-dimethyl-1,1'-ditrithyl-4,4'-biimidazole)-nitrato-copper(II)] acetonitrile solvate [20] and bis-{[μ_2-2,6-bis(3-piridiloxi)pyrazine]-(μ_2-nitrato)-nitrato-copper(II)}acetonitrile solvate [21]. These distances are in the range 2.360(2)–2.403(3) Å for the longer Cu–(ONO$_2$)$_{bridge}$ length and 1.975(2)–2.011(4) Å for the shorter one. The Cu–(ONO$_2$)$_{terminal}$ bond distance is slightly shorter than the corresponding ones in the aforementioned compounds [1.963(2)–2.009(3) Å]. The Cu–N$_{pyrazole}$ in **2** and **3** are comparable to the

Table 3. Selected bond distances (Å) and angles (°) for **2** and **3**.

	2	**3**
Cu–N(1)	1.978(3)	1.979(2)
Cu–N(3)	1.977(3)	1.992(2)
Cu–O(1)	1.952(2)	1.956(1)
Cu–O(2)		2.808(2)
Cu–O(4)	2.001(2)	1.960(1)
Cu–O(6)	2.727(2)	
Cu–O(4^i)		2.421(1)
Cu–O(5^i)	2.380(2)	
N(1)–Cu–N(3)	80.7(1)	80.8(1)
N(1)–Cu–O(1)	172.1(1)	98.1(1)
N(1)–Cu–O(2)		82.5(1)
N(1)–Cu–O(4)	92.4(1)	167.1(1)
N(1)–Cu–O(4^i)		94.1(1)
N(1)–Cu–O(5^i)	86.6(1)	
N(1)–Cu–O(6)	85.7(1)	
N(3)–Cu–O(1)	98.9(1)	178.9(1)
N(3)–Cu–O(2)		128.7(1)
N(3)–Cu–O(4)	162.9(1)	94.1(1)
N(3)–Cu–O(4^i)		94.0(1)
N(3)–Cu–O(5^i)	115.0(1)	
N(3)–Cu–O(6)	111.4(1)	
O(1)–Cu–O(2)		50.8(5)
O(1)–Cu–O(4)	85.9(1)	87.0(1)
O(1)–Cu–O(6)	87.2(1)	
O(1)–Cu–O(4^i)		86.4(1)
O(1)–Cu–O(5^i)	100.6(1)	
O(2)–Cu–O(4)		109.7(1)
O(2)–Cu–O(4^i)		135.5(1)
O(4)–Cu–O(6)	52.2(1)	
O(4)–Cu–O(4^i)		74.3(1)
O(4)–Cu–O(5^i)	79.8(1)	
O(6)–Cu–O(5^i)	130.9(1)	

Symmetry codes: ^{i}−1/2 + x, 1/2 − y, −z for **2** and 1 − x, 1 − y, 2 − z for **3**.

average value [1.972(47) Å] calculated for 30 Cu(II) complexes with the CuN_2O_3 chromophore. Finally, the Cu–N$_{thiazine}$ bond lengths in **1**–**3** are similar to the five complexes with this type of bond found in CSD: bis(μ_2-cloro)-dichloro-bis(2-(2-pyridilamine)-5,6-dihydro-4H-1,3-thiazine-*N*,*N*′)-di-copper(II) [2.001(3) Å] [22], (nitrato-O)-bis(2-(2-pyridil)amine-5,6-dihydro-4H-1,3-thiazine)-copper(II) nitrate [1.968(2) Å] [23], dichloro-(5,5′,6,6′-tetrahydro-2,2′-bi-4H-1,3-thiazine-N^3,N$^{3\prime}$)-copper(II) [2.013(5) Å] [24], bis(μ_2-chloro)-chloro-(5,5′,6,6′-tetrahydro-2,2′-bi-4H-1,3-thiazine-N^3,N$^{3\prime}$)-copper(II) [2.052(3) Å and 2.005(5) Å] [24], and dichloro-(3,4-dichloro-N-(3-5,6-dihydro-4H-1,3-thiazin-2-yl)-1,3-thiazolidin-2-ylidene)aniline-N)-copper(II) [1.89(3) Å] [2].

The supramolecular structure in **1** is stabilized by a hydrogen-bond network (figure 4 and table 2) where water molecules are hydrogen donors and nitrates are hydrogen acceptors. Aromatic CH···π interactions between the pyrazole rings which contribute to the crystal packing have been detected in such a way that these rings act both as C–H donors and π acceptors. These interactions are represented in figure 4. In **2** and **3,** molecules are linked by van der Waals forces, but in **3** CH···π T-shaped aromatic interactions between the phenyl rings also appear (figure 5).
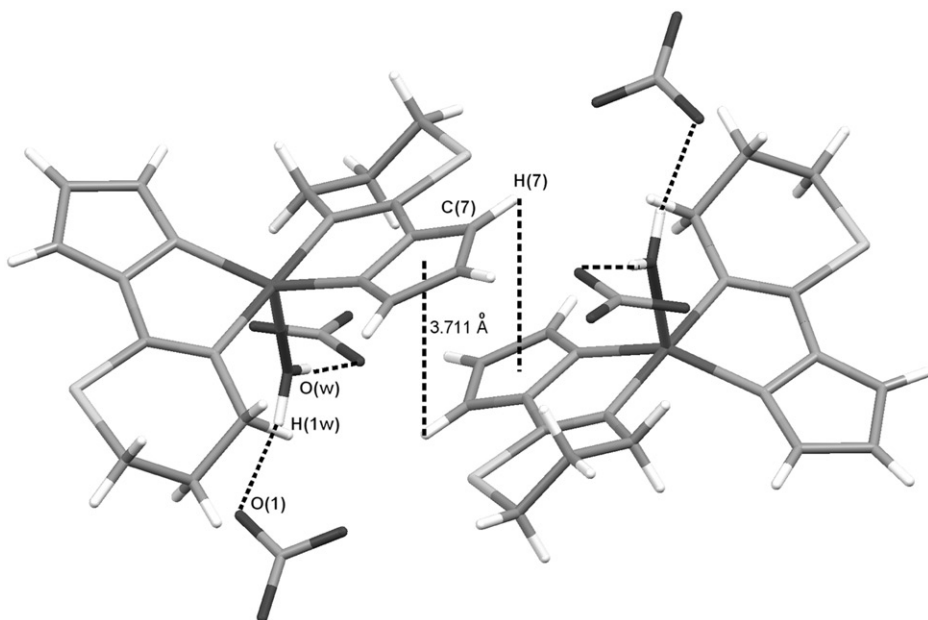
P. Torres-García et al.

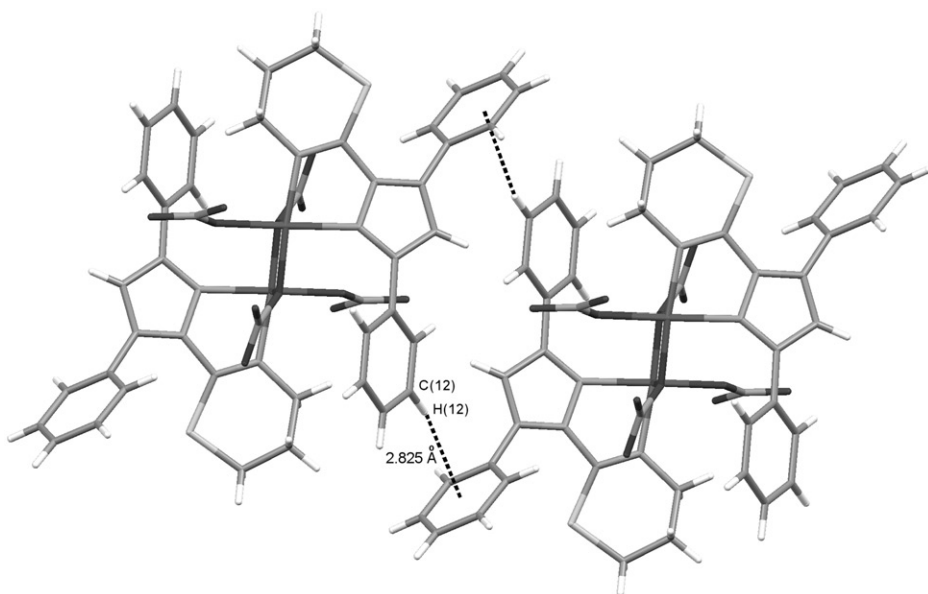Figure 4. Hydrogen bonds and aromatic interactions in the crystal of **1**.

Figure 5. Aromatic interactions in the crystal of **3**.

Table 4. IR spectral assignments (cm^{-1}) for **1–3**, PzTz, DMPzTz, and DPhPzTz.

	1	PzTz	**2**	DMPzTz	**3**	DPhPzTz
ν(C=N)	1606(vs)	1635(vs)	1602(s)	1639(s)	1614(s)	1639(vs)
Pyrazole ring vibrations	1527(s)	1510(m)	1565(s)	1566(m)	1554(m)	1548(w)
	1382(vs)	1386(s)	1422(sh)	1411(m)	1411(m)	1406(m)
	1324(vs)	1327(vs)	1382(vs)	1375(s)	1311(s)	1303(m)
ν(Cu–ONO$_2$)			311(w)		319(w)	
			328(w)		345(w)	
ν(Cu–O$_{water}$)	359(w)					
ν(Cu–N$_{pyrazole}$)	300(w)		283(w)		287(w)	
ν(Cu–N$_{thiazine}$)	263(w)		247(w)		251(w)	

sh = shoulder, w = weak, m = medium, s = strong, vs = very strong.

Table 5. EPR parameters for **1–3**.

	$g_{\parallel}$	$g_{\perp}$	g_1	g_2	g_3	G	R
1			2.220	2.120	2.028		1.09
2	2.235	2.077				3.05	
3			2.334	2.062	1.882		0.66

3.2. *Spectroscopic studies*

Reflectance spectra of **1–3** present an asymmetric broad band centered at 12,690 cm^{-1} for **1**, 14,290 cm^{-1} for **2**, and 15,020 cm^{-1} for **3**. Presumably, d–d transitions are responsible for these bands [25]. The spectra also display strong absorptions that can be assigned to Cu $\rightarrow$ ligand charge transfer bands [26, 27] and $\pi \rightarrow \pi^*$ transitions from the organic ligands [3]. Specifically, these bands appear at 37,040 and 28,740 (shoulder) cm^{-1} for **1**, 37,170 cm^{-1} for **2**, and 34,360 and 25,060 (shoulder) cm^{-1} for **3**. The most relevant bands in the IR spectra of **1–3** and the organic ligands are listed in table 4. There is a shift to lower frequencies for the bands assigned to thiazine ring vibrations, whereas bands attributable to pyrazole ring vibrations suffer a shift in the opposite direction. These facts confirm coordination through the pyrazole and thiazine nitrogen atoms [28–30].

Coordination modes of nitrate can be determined using the method proposed by Lever *et al.* [31], which is based on the pattern of the splitting of the ($\nu_1 + \nu_4$) combination bands. Thus, in the spectrum of **2** two ($\nu_1 + \nu_4$) bands are detected at 1764 and 1737 cm^{-1}. The value of the splitting ($\Delta = 27$ cm^{-1}) fits with a bidentate nitrate, according to Lever's criteria. The presence of two bands at 1731 and 1714 cm^{-1} ($\Delta = 17$ cm^{-1}) for **3** are indicative of a nitrate that behaves as intermediate between mono and bidentate.

In the 500–150 cm^{-1} region of spectra, several bands corresponding to metal–ligand stretching vibrations are detected. The ν(Cu–ONO$_2$) vibrations are registered at 255–325 cm^{-1} [32, 33], the ν(Cu–O$_{water}$) signal appears above 350 cm^{-1} [16, 32] and the ν(Cu–N$_{pyrazole}$) vibration is detected at 226–315 cm^{-1} [34–36]. Finally, the signal corresponding to ν(Cu–N$_{thiazine}$) is usually detected at 250–265 cm^{-1} [22, 37].

The EPR spectra of polycrystalline samples at 298 K of **1–3** were recorded in the X-band using 100 kHz field modulation. EPR parameters are presented in table 5.

Compound **1** exhibits a rhombic spectrum with a value for R $[R = (g_2 - g_1)/(g_3 - g_2)]$ close to 1, thus the ground state of the unpaired electron cannot be determined from this experiment [38]. The spectrum of **2** is typically axial with well-defined $g_\parallel$ and $g_\perp$ values. The geometric parameter G $[G = (g_\parallel - 2)/(g_\perp - 2)]$ is in the range 3.0–6.0 and $g_\parallel > g_\perp > 2.0023$, thus indicating that the unpaired electron is located in a $d_{x^2-y^2}$ orbital associated with square-pyramidal stereochemistry, in agreement with the crystallographic data [39, 40]. Finally, the EPR spectrum of **3** is rhombic, exhibiting a broad and weak feature at 2260–2740 G ($g_3 = 2.334$), a relatively strong signal at 3000 G ($g_2 = 2.062$), and a valley at 3730 G ($g_1 = 1.882$). These features correspond to $\Delta m_s = \pm 1$ transitions for an $S = 1$ dinuclear copper(II) complex. A weak absorption at 1600 G is assigned to $\Delta m_s = \pm 2$ transitions and a feature at 3350 G is attributed to a monomeric Cu(II) impurity. The geometric parameter R is consistent with a square-pyramidal geometry with a $d_{x^2-y^2}$ ground state [25, 39].

3.3. *Magnetic properties*

The observed molar magnetic susceptibility for **1** was corrected for diamagnetism and temperature-independent paramagnetism to provide the fully corrected magnetic moment at room temperature of 1.83 BM, in the range 1.75–2.20 BM typical for mononuclear copper(II) complexes without Cu–Cu interactions, regardless of the stereochemistry and independent of temperature, except at extremely low temperatures (<5 K) [41].

Variable temperature (7.5–300 K) magnetic susceptibility data were collected for polycrystalline samples of **2** and **3**. The high-temperature data ($T > 140$ K) were fit to a Curie–Weiss relationship, yielding $C = 0.42$ cm^3 mol^{-1} K and $\theta = 0.97$ K for **2** and $C = 0.88$ cm^3 mol^{-1} K and $\theta = -0.70$ K for **3**, which indicate weak ferromagnetic and antiferromagnetic interactions between copper(II) ions. The corrected magnetic moments measured were 1.83 BM for **2** and 1.91 BM for **3**. Susceptibility values per mole of monomer as a function of temperature in the form of χ_M and $\chi_M T$ for **2** have been plotted in figure 6. The magnetic susceptibility data were analyzed in terms of the polynomial expression (1) reported by Baker *et al.* [42] for linear chains with ferromagnetic coupling.

$$\chi_M chain = \frac{N g^2 \mu_B^2}{4 K_B T} \left[\frac{1 + Ax + Bx^2 + Cx^3 + Dx^4 + Ex^5}{1 + A'x + B'x^2 + C'x^3 + D'x^4} \right]^{2/3}. \tag{1}$$

In this expression, $x = J/K_B T$ and the constants A–D' have the following values: $A = 5.7979916$, $B = 16.902653$, $C = 29.376885$, $D = 29.832959$, $E = 14.036918$, $A' = 2.7979916$, $B' = 7.0086780$, $C' = 8.6538644$, $D' = 4.5743114$. Moreover, equation (1) can be corrected to consider interaction between chains in the crystal [43, 44]:

$$\chi_M = \frac{\chi_M chain}{1 - \frac{zJ' \chi_M chain}{N g^2 \mu^2}}. \tag{2}$$

The best fit gives $g = 2.13$, $J = 0.34$ cm^{-1} mol^{-1}, and $R = 1.03 \times 10^{-8}$ using equation (1) and $g = 2.13$, $J = 0.33$ cm^{-1} mol^{-1}, $zJ' = 0.004$ cm^{-1} mol^{-1}, and $R = 9.58 \times 10^{-9}$ using equation (2) $[R = \Sigma(\chi_{Mj}^{obs} - \chi_{Mj}^{cal})^2 / \Sigma(\chi_{Mj}^{obs})^2]$. Thus, the goodness of fit is similar with both equations. The low value of the coupling constant J indicates a weak
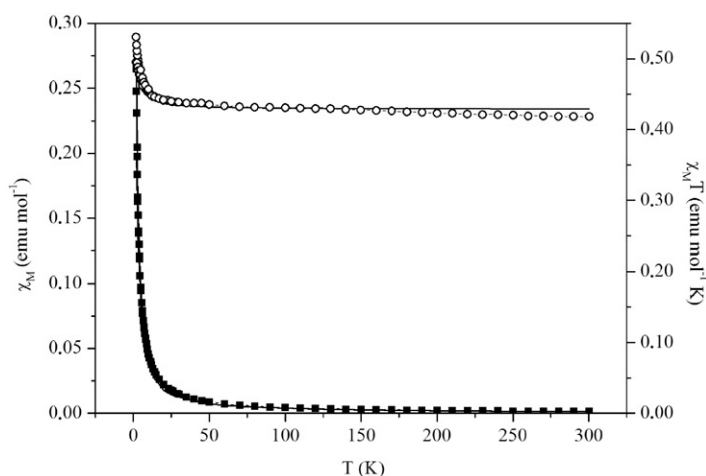
Figure 6. χ_M *vs.* T (■) and $\chi_M T$ *vs.* T (○) plot for **2**. The solid line represents the best fit of the data with the model described in the text.
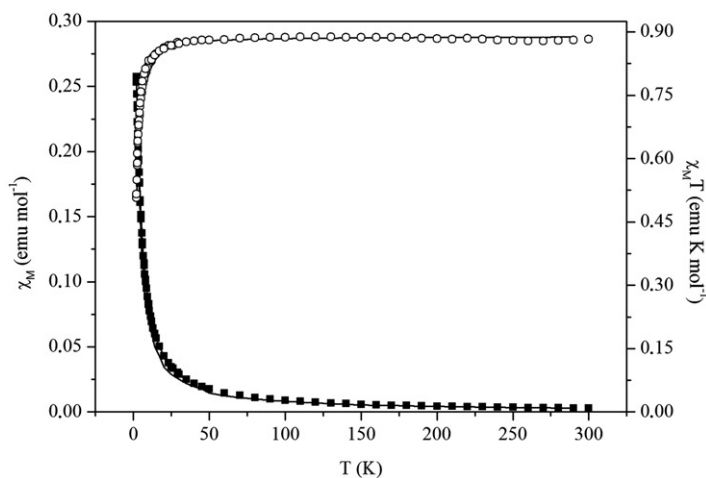

Figure 7. χ_M *vs.* T (■) and $\chi_M T$ *vs.* T (○) plot for **3**. Solid lines represent the best fit of the data with the model described in the text.

ferromagnetic coupling between copper(II) atoms in a chain. Likewise, since the value of zJ' obtained with equation (2) is very low, we can consider that the interaction between different chains in the crystal is negligible.

On the other hand, the temperature dependence of the magnetic susceptibility per mole of dimer (χ_M and $\chi_M T$) for **3** is shown in figure 7. The experimental data were fitted using the Bleaney–Bowers equation (3) for a binuclear compound modified to take into account paramagnetic impurities [45], according to the EPR data.

$$\chi_M = \frac{2Ng^2\mu_B^2}{K_B T[3 + \exp(-2J/K_B T)]}(1-\rho) + \frac{2Ng^2\mu_B^2}{2K_B T}\rho. \tag{3}$$

In this expression ρ is the amount of paramagnetic impurities. The parameters J, g, and ρ were determined as adjustable parameters in a least-squares fitting procedure that led to the values $J = -1.30\,\text{cm}^{-1}$, $g = 2.19$, and $\rho = 0.27$ with an agreement factor $R = 6.40 \times 10^{-10}$. The negative and small value of the coupling constant J indicates a weak antiferromagnetic interaction.

4. Conclusion

We have synthesized and structurally characterized three new Cu(II) complexes: $[\text{Cu}(\text{H}_2\text{O})(\text{PzTz})_2](\text{NO}_3)_2$ (**1**), $[\text{Cu}(\text{DMPzTz})(\mu\text{-NO}_3)(\text{NO}_3)]_n$ (**2**), and $[\{\text{Cu}(\text{NO}_3)(\text{DPhPzTz})\}_2(\mu\text{-NO}_3)_2]$ (**3**). According to the X-ray data, the size of the ligands influences coordination. Thus, in **1** the Cu(II) is coordinated to two bidentate ligands, whereas in **2** and **3** only one ligand is bonded to the metal even when the stoichiometry of synthesis reactions was 1 : 2 (metal : organic ligand). This is probably a consequence of the strain introduced by the methyl and phenyl substituents in DMPzTz and DPhPzTz, respectively, which obstruct coordination of two voluminous ligands to copper(II) and forces copper to incorporate nitrate in order to complete the five-coordination. By comparing **2** and **3**, it can be observed that the distance between two copper(II) ions is longer in **2** (5.069 Å) than in **3** (3.503 Å), which could be a consequence of higher steric hindrance induced by the methyl groups than phenyl rings, because phenyl rings can rotate around the σ bond with pyrazole and adopt a position that minimizes steric effects. This fact determines the coordination mode of bridging nitrates, which is μ-1,2 for **2** and μ-1,1 for **3**.

Supplementary material

CCDC 878 087 (**1**), 878 088 (**2**), and 878 089 (**3**) contain the supplementary crystallographic data for this article. These data can be obtained free of charge *via* www.ccdc.cam.ac.uk/conts/retrieving.html (or from the CCDC, 12 Union Road, Cambridge CB2 1EZ, UK; Fax: +44 1 223 336 033; E-mail: deposit@ccdc.cam.ac.uk).

Acknowledgments

References

[1] B. Gómez-Lor, E. Gutiérrez-Puebla, M. Iglesias, M.A. Monge, C. Ruiz-Valero, N. Snejko. *Inorg. Chem.*, **41**, 2429 (2002).
[2] A.M. Lozano-Vila, F. Luna-Giles, E. Viñuelas-Zahínos, F.L. Cumbrera, A.L. Ortiz, F.J. Barros-García. *Polyhedron*, **30**, 1157 (2011).

[3] P. Torres-García, E. Viñuelas-Zahínos, F. Luna-Giles, J. Espino, F.J. Barros-García. *Polyhedron*, **30**, 2627 (2011).

[4] P. Torres-García, R. Pedrero-Marín, F. Luna-Giles, E. Viñuelas-Zahínos, F.J. Barros-García. *J. Coord. Chem.*, **64**, 3887 (2011).

[5] P. Torres-García, R. Pedrero-Marín, F. Luna-Giles, A.V. Huertas-Sánchez, E. Viñuelas-Zahínos. *Polyhedron*, **31**, 307 (2012).

[6] Bruker AXS Inc. *SADABS, version 2.03*, Bruker AXS Inc., Madison, WI, USA (2001).

[7] G.M. Sheldrick. *SHELXS-97, Program for Crystal Structures Solution*, University of Göttingen, Germany (1997).

[8] G.M. Sheldrick. *SHELXL-97, Program for Crystal Structures Refinement*, University of Göttingen, Germany (1997).

[9] L.J. Farrugia. *J. Appl. Cryst.*, **32**, 837 (1999).

[10] L.J. Farrugia. *J. Appl. Cryst.*, **30**, 565 (1997).

[11] C.F. Macrae, I.J. Bruno, J.A. Chisholm, P.R. Edgington, P. McCabe, E. Pidcock, L. Rodriguez-Monge, R. Taylor, J. van de Streek, P.A. Wood. *J. Appl. Crystallogr.*, **41**, 466 (2008).

[12] A.W. Addison, T.N. Rao, J. Reedijk, J. van Rijn, G.C. Verschoor. *J. Chem. Soc., Dalton Trans.*, 1349 (1984).

[13] E.L. Muetterties, J. Guggemberger. *J. Am. Chem. Soc.*, **96**, 1748 (1974).

[14] W. Fitzgerald, B.J. Hathaway. *J. Chem. Soc., Dalton Trans.*, 567 (1981).

[15] R. Ballesteros, B. Abarca, A. Samadi, J. Server-Carrió, E. Escrivá. *Polyhedron*, **18**, 3129 (1999).

[16] M.A. Maldonado-Rogado, E. Viñuelas-Zahínos, F. Luna-Giles, A. Bernalte-García. *Polyhedron*, **26**, 1137 (2007).

[17] I.J. Bruno, J.C. Cole, P.R. Eddington, M. Kessler, C.F. Macrae, P. McCabe, J. Pearson, R. Taylor. *Acta Crystallogr.*, **B58**, 389 (2002).

[18] H. Casellas, P. Gámez, J. Reedijk, I. Mutikainen, U. Terpeinen, W. Masciocchi, S. Galli, A. Sironi. *Inorg. Chem.*, **44**, 7918 (2005).

[19] P. Gámez, P. de Hoog, O. Roubean, M. Lutz, W.L. Driessen, A.L. Spek, J. Reedijk. *Chem. Commun.*, 1488 (2002).

[20] G. Aromí, P. Gámez, H. Koijman, A.L. Spek, W.L. Driessen, J. Reedijk. *Eur. J. Inorg. Chem.*, **2003**, 1394 (2003).

[21] D.A. McMorran, P.J. Steel. *J. Chem. Soc., Dalton Trans.*, 3321 (2002).

[22] A. Bernalte-García, F.J. Barros-García, F.J. Higes-Rolando, F. Luna-Giles, R. Pedrero-Marín. *J. Inorg. Biochem.*, **98**, 15 (2004).

[23] M.C. García-Cuesta, A.M. Lozano, J.J. Meléndez-Martínez, F. Luna-Giles, A.L. Ortiz, L.M. González-Méndez, F.L. Cumbrera. *J. Appl. Crystallogr.*, **37**, 993 (2004).

[24] S.F. Hadad, J. Pickardt. *Transition Met. Chem.*, **18**, 377 (1993).

[25] J. Hathaway. In *Comprehensive Coordination Chemistry*, G. Wilkinson (Ed.), Vol. 5, pp. 662–668, Pergamon Press, Oxford (1987).

[26] E. Viñuelas-Zahínos, F. Luna-Giles, P. Torres-García, A. Bernalte-García. *Polyhedron*, **28**, 4056 (2009).

[27] A.M. Schuitema, A.F. Stassen, W.L. Driessen, J. Reedijk. *Inorg. Chim. Acta*, **337**, 48 (2002).

[28] M. Shakir, S.P. Vakey, F. Firdaus, P.S. Hameed. *Polyhedron*, **13**, 2319 (1994).

[29] B. Singh, R.N. Singh, R.C. Aggarwal. *Polyhedron*, **4**, 401 (1985).

[30] M.G. Abd El-Wahed, M.S. Refat, S.M. El-Megharbel. *J. Mol. Struct.*, **888**, 416 (2008).

[31] A.B.P. Lever, E. Mantovani, B.S. Ramaswamy. *Can. J. Chem.*, **49**, 1957 (1971).

[32] F.J. Barros-García, A. Bernalte-García, F.J. Higes-Rolando, F. Luna-Giles, M.A. Maldonado-Rogado, E. Viñuelas-Zahínos. *Inorg. Chim. Acta*, **357**, 3574 (2004).

[33] K. Fujisawa, Y. Ishikawa, Y. Miyashita, K. Okamoto. *Inorg. Chim. Acta*, **363**, 2977 (2010).

[34] J. Pons, A. Chadghan, J. Casabó, A. Álvarez-Larena, J.F. Piniella, J. Ros. *Polyhedron*, **20**, 2531 (2001).

[35] D. Nemcsok, A. Kovács, K.M. Szécsényi, V.M. Leovac. *Chem. Phys.*, **328**, 85 (2006).

[36] J. Reedijk. *Inorg. Chim. Acta*, **3**, 517 (1969).

[37] J. Nelson, S. Martin-Nelson, W.D. Perry. *J. Chem. Soc., Dalton Trans.*, 1282 (1976).

[38] V. Philip, V. Suni, M.R.P. Kurup, M. Nethaji. *Polyhedron*, **24**, 1133 (2005).

[39] B.J. Hathaway. *J. Chem. Soc., Dalton Trans.*, 1196 (1972).

[40] J. Garcia-Tojal, L. Lezama, J.L. Pizarro, M. Insausti, M.I. Arriortua, T. Rojo. *Polyhedron*, **18**, 3703 (1999).

[41] G. Albertin, E. Bordignon, A.A. Orio. *Inorg. Chem.*, **14**, 1411 (1975).

[42] G.A. Baker, G.S. Rushbrooke, H.E. Gilbert. *Phys. Rev. A*, **135**, 1272 (1964).

[43] B.N. Figgis, R.L. Martin. *J. Chem. Soc.*, 3837 (1956).

[44] W.E. Hatfield. *Comments Inorg. Chem.*, **1**, 105 (1981).

[45] B. Bleaney, K.D. Bowers. *Proc. R. Soc. London Ser. A*, **214**, 451 (1952).